

Translational symmetry breaking in the electronic nematic phase of BaFe_2As_2

K. Koshiishi,¹ L. Liu,¹ K. Okazaki,^{1,2} H. Suzuki,^{1,3,4} J. Xu,¹ M. Horio,^{1,2} H. Kumigashira,^{5,3} K. Ono,^{5,6} M. Nakajima,^{7,8,9} S. Ishida,⁷ K. Kihou,⁷ C. H. Lee,⁷ A. Iyo,⁷ H. Eisaki,⁷ S. Uchida,^{1,7} and A. Fujimori^{1,10,*}

¹Department of Physics, The University of Tokyo, Bunkyo-ku, Tokyo 113-0033, Japan

²Institute for Solid State Physics, The University of Tokyo, Kashiwa, Chiba 277-8581, Japan

³Institute of Multidisciplinary Research for Advanced Materials (IMRAM), Tohoku University, Sendai 980-8577, Japan

⁴Frontier Research Institute for Interdisciplinary Sciences, Tohoku University, Sendai 980-8578, Japan

⁵KEK, Photon Factory, Tsukuba, Ibaraki 305-0801, Japan

⁶Department of Applied Physics, Osaka University, Suita 565-0871, Osaka, Japan

⁷National Institute of Advanced Industrial Science and Technology, Tsukuba, Ibaraki, 305-8568, Japan

⁸RIKEN Center for Emergent Matter Science, Wako, Saitama 351-0198, Japan

⁹Department of Physics, Osaka University, Toyonaka, Osaka 560-0043, Japan

¹⁰Department of Physics, National Tsing Hua University, Hsinchu 300044, Taiwan

(Dated: December 3, 2025)

The microscopic origin of the nematicity, namely, four-fold rotational symmetry breaking in iron-based superconductors has been controversial since its discovery. In particular, its relationship with the stripe-type spin-density-wave order and the orthorhombic lattice distortion in the antiferromagnetic orthorhombic (AFO) phase, which exists at temperatures below the electronic nematic phase, has been highly debated. Here, we report on the temperature evolution of angle-resolved photoemission spectra of the parent compound BaFe_2As_2 , ranging from the AFO to nematic to paramagnetic phases. The Dirac cone feature, which is formed in the AFO phase, is found to persist in the nematic phase, suggesting that an antiferroic order of the same periodicity as the AFO phase persists in the nematic phase. Considering the relatively shallow d_{xy} orbital in BaFe_2As_2 , we propose that an antiferro-orbital order involving the d_{xy} and other orbitals takes place in the nematic phase.

I. INTRODUCTION

The parent compounds of a majority of iron-based superconductors (FeSCs) are antiferromagnetic (AFM) metals with a stripe-type spin-density wave (SDW) order accompanied by a tetragonal-to-orthorhombic lattice distortion. Figure 1(a) shows the crystal and magnetic structures of BaFe_2As_2 , one of the parent compounds of the so-called 122-type FeSCs. Below $T_N = T_s$ (T_N : Néel temperature; T_s : structural transition temperature), the system enters the antiferromagnetic-orthorhombic (AFO) phase [1]. Carrier doping or chemical pressure by element substitution for BaFe_2As_2 (e.g., K for Ba; Co, Ni, or Cu for Fe; As for P) suppresses the AFO order and superconductivity emerges [2–6], as shown in the phase diagram [Fig. 1(b)]. Above the AFO and the superconducting (SC) phases up to the temperature denoted by T^* in the figure, there appears the so-called electronic nematic phase [7]. In that phase, although the crystal lattice recovers the tetragonal symmetry, the electronic system still exhibits the broken four-fold rotational symmetry (C_4 symmetry) but shows a two-fold rotational one (C_2 symmetry).

In the AFO phase, the SDW has the magnetic ordering wave vector of $\mathbf{Q} = (\frac{1}{2}, 0, \frac{1}{2})$ in r.l.u. and the magnetic moments at the Fe sites are aligned ferromagnetically along the orthorhombic b axis and antiferromagnetically along the orthorhombic a axis and along the c axis. The lattice constant along the b -axis is slightly smaller than that along the a -axis. In the paramagnetic (PM) phase, the tetragonal $I4/mmm$ symmetry is recovered and the body-centered-tetragonal (bct)

unit cell contains two Fe atoms. In the stripe-type SDW phase below $T_N = T_s \sim 140$ K, the unit cell of orthorhombic $Fmmm$ symmetry [Fig. 1 (a)] contains four Fe atoms. Correspondingly, the Brillouin-zone of the bct lattice is folded below $T_N = T_s$, as shown in Fig. 2(c). In fact, the Fermi surface reconstruction [Fig. 2(e)] and the folded band structure shown in have been identified by angle-resolved photoemission spectroscopy (ARPES) studies of BaFe_2As_2 [8–10].

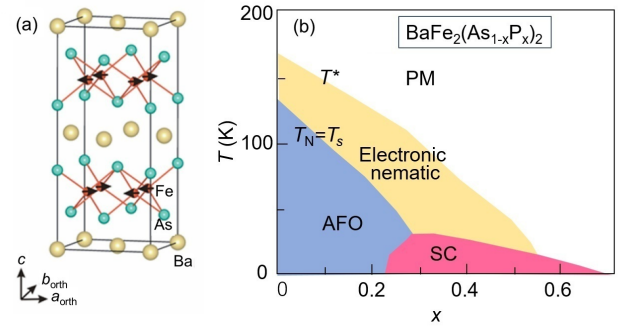


FIG. 1. (a) Crystal and magnetic structures of the 122-type BaFe_2As_2 in the antiferromagnetic orthorhombic (AFO) phase (adopted from Ref. 1). (b) Phase diagram of the P-substituted BaFe_2As_2 [7]. PM: Paramagnetic phase; SC: Superconducting phase; T_N : Néel temperature; T_s : Tetragonal-to-orthorhombic transition temperature; T^* : Nematic transition temperature.

It has been known that, in the 122-type compounds, twinned domains are formed below the structural phase transition temperature T_s , but by applying uniaxial pressure, one can avoid the twinning [11]. In the AFO phase, detwinned single crystals of the 122-type FeSCs have revealed the intrinsic in-plane anisotropy of the electronic structure detected

* fujimori@phys.s.u-tokyo.ac.jp

by transport [11, 12], optical conductivity [13, 14], neutron scattering [15], and ARPES [10, 16] measurements. Furthermore, in some of these measurements, the same in-plane anisotropies continue up to a few to several tens degree above T_s [11, 12, 16–18]. Such behaviors where the electronic states exhibit spontaneously broken four-fold rotational symmetry are called electronic nematicity in analogy to an ordered phase of liquid crystals. Evidence for the electronic nematicity above the structural transition temperature T_s has also been found in single domain samples of $\text{BaFe}_2(\text{As}_{1-x}\text{P}_x)_2$ through magnetic torque measurements, as shown in Fig. 1(b) [7]. This anomaly is seen up to $\sim T^*$ through the finite amplitude of two-fold symmetry signals in magnetic torque. In the ARPES study of detwinned $\text{Ba}(\text{Fe}_{0.975}\text{Co}_{0.025})_2\text{As}_2$ [16], too, it has been reported that the in-plane anisotropy of the band structure persists above T_s . Nematicity above T_s has also been observed in transport and optical measurements [12, 14]. In other strongly correlated electron systems such as cuprate high-temperature superconductors [19–21] and heavy fermion systems [22], too, nematicity has been reported. Recently, the electronic nematicity in the 11-type FeSCs such as FeSe [23] is more extensively studied because they do not show AFM order and have simpler phase diagrams.

Since FeSCs are multi-band systems, the orbital degrees of freedom is considered to play an important role. Theoretically, a ferro-orbital order is proposed as an origin of the broken C_4 -symmetry in iron pnictides [24]. On the other hand, no anomalies in the elastic constant C_{66} have been observed at T^* in ultrasonic measurements [25], implying that no transition to ferro-orbital order occurs at T^* . In this regard, an antiferro-orbital order has been proposed by Kontani *et al.* [26]. Antiferro-quadrupole fluctuations induced by electron-phonon interaction may lead to an antiferro-orbital order in the electronic nematic phase of BaFe_2As_2 that can hardly be detected by long-wavelength ($\mathbf{q} \simeq 0$) probes such as the C_{66} measurements.

In the present paper, we report on an ARPES study of detwinned BaFe_2As_2 crystals to reveal the temperature evolution of band-folding features from the AFO phase to the electronic nematic to paramagnetic (PM) tetragonal phases. We find that a Dirac-cone feature near the X point of the original Brillouin zone, which is created by the AFM band folding due to the SDW order, persists above $T_N \simeq T_s = 142$ K up to $T^* \sim 170$ K. Our results indicate that the band folding persists in the electronic nematic phase even after the AFM order vanishes above $T_s = T_N$, suggesting that the nematic phase has the same periodicity as the stripe-type SDW order. Although the nature of the ordering cannot be uniquely determined by ARPES alone, the present results demonstrate that an antiferro-ordered phase persists above T_s up to T^* in BaFe_2As_2 .

II. METHODS

High-quality single crystals of BaFe_2As_2 ($T_N \simeq T_s = 142$ K) were grown by the self-flux method followed by annealing [12, 13, 17]. In order to detect the anisotropic electronic

structure by ARPES measurements, we detwinned the single crystals of BaFe_2As_2 by applying uniaxial strain using a specially designed sample holders similar to that used in Ref. 27. ARPES measurements were performed at beamline 28A of Photon Factory, High-Energy Accelerator Research Organization (KEK) using a SCIENTA SES-2002 electron analyzer. The total energy resolution was set to ~ 20 meV. ARPES spectra were obtained using circularly-polarized light with the photon energy of 63 eV, corresponding to $k_z \sim 2\pi/c$. The crystals were cleaved *in situ* at 20 K for low-temperature measurements and at 100 K for temperature-dependent measurements. The measurements were carried out in an ultrahigh vacuum of $\sim 4 \times 10^{-10}$ Torr. The Fermi level (E_F) of the samples was calibrated using gold.

Density-functional-theory (DFT) calculations using the full-potential linearized augmented plane-wave (FP-LAPW) method were performed with a WIEN2k package [28]. The effective potential is calculated using the generalized gradient approximation (GGA-PBE). The experimental lattice parameters of $\text{Ba}_{0.6}\text{K}_{0.4}\text{Fe}_2\text{As}_2$ with the tetragonal $I4/mmm$ structure [29] were used.

III. RESULTS AND DISCUSSION

First, in order to confirm whether the samples were sufficiently detwinned or not, we performed ARPES measurements on both twinned and detwinned samples in the AFO phase. Figures 2(a) and 2(b) show Fermi surface (FS) mapping in the k_x - k_y planes of the detwinned and twinned samples, respectively. The geometry of the FSs of the twinned sample [panel (b)] approximately show four-folded rotational symmetry around the Z point and the ZX and ZY directions are similar. On the other hand, for the detwinned BaFe_2As_2 [panel (a)], differences of the FSs around the Z-X and Z-Y lines can be clearly seen as already reported in Ref. 10, i.e., the FSs of the detwinned sample show two-fold rotational symmetry. For example, bright small spots around the Y point observed in the twinned sample disappear in the detwinned sample, which is consistent with the previous ARPES study [16].

In Fig. 2(c), the three-dimensional Brillouin zone (BZ) of the PM state and the AFM state are depicted by gray and green lines, respectively. In the PM phase, the BZ has four-fold rotational symmetry around the Γ -Z line and the X and Y points are equivalent. In the AFO phase, because of the stripe-type order of the magnetic moments at the Fe sites, the unit cell is doubled and contains four Fe atoms. Hence, the energy bands and FSs of the PM phase are folded into the AFM BZ of half volume. In addition, the Z(Γ) point should be equivalent to the Y(X) point but non-equivalent to the X(Y) point in the AFM BZ as shown in Fig. 2(d). In Fig. 2(a), FSs around the Z point are similar to those around the Y point while they are different from those around the X point, suggesting that FSs intrinsic to the AFO phase were observed and hence that the crystals were properly detwinned.

Focusing on the geometry of the FSs in the AFO phase, we found that they consist of a circular hole pocket centered at the center of the AFM BZ, two elliptical electron pocket

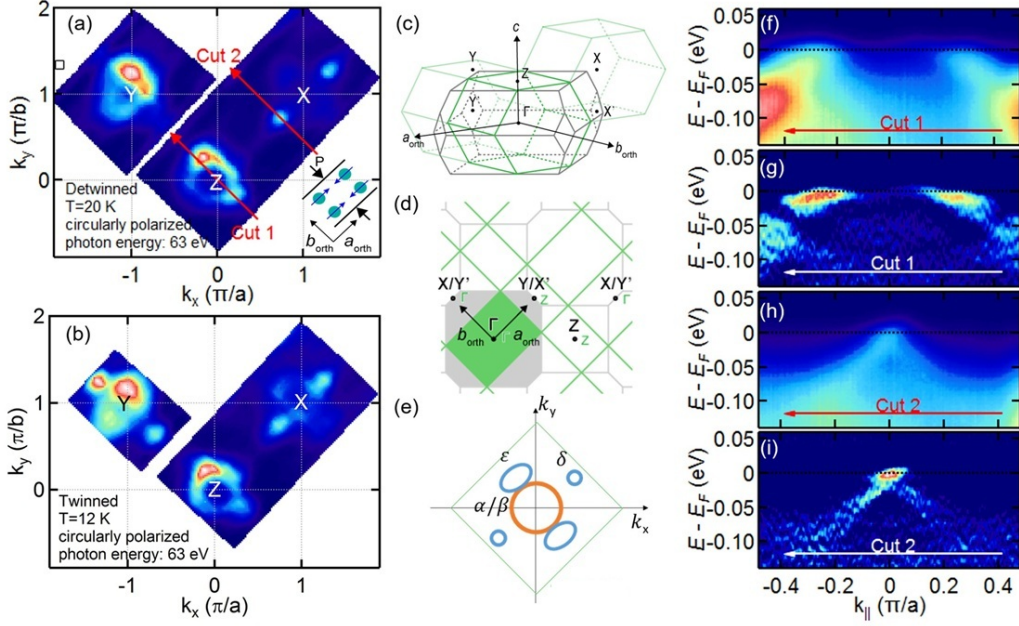


FIG. 2. ARPES spectra of BaFe_2As_2 in the antiferromagnetic-orthorhombic phase. (a), (b) Fermi surface mapping for the detwinned and twinned BaFe_2As_2 crystals, respectively. Inset to (a) shows the crystal and magnetic structure on the 2D plane and the direction of the applied strain P . (c) 3D Brillouin zones of the PM (gray) and AFO (green) phases. (d) Corresponding in-plane 2D Brillouin zones. (e) Schematic Fermi surfaces. Orange and blue circles indicate hole pockets and electron pockets, respectively. (f), (h) Energy-momentum plots along cuts 1 and 2 indicated by red arrows in (a). (g), (i) Second-derivative plots of EDCs corresponding to cut 1 and cut 2.

ets next to the hole pocket on the Z-Y line, and two high-intensity tiny electron pockets on the Z-X line, which correspond to the apex of the Dirac cone as reported in Ref. 30, denoted as α/β , ϵ , and δ , respectively. A schematic figure of the FSs in the AFO phase we have observed are shown in Fig. 2(e). The orange and blue circles correspond to hole and electron Fermi surfaces, respectively. Terashima *et al.* [31] have also determined the Fermi surfaces similar to our results by Shubnikov-de Hass oscillation measurements [32]. Such elliptical electron pockets and tiny electron pockets should not be seen in the PM phase, where three hole FSs around the Γ point and two electron FSs around the zone corner exist. Thus, the observed FS features are characteristics of the AFO phase with the Fermi-surface reconstruction caused by the stripe-type SDW.

Binding energy (E_B) versus momentum (\mathbf{k}) plots across the hole and electron pockets along cuts 1 and 2 [red arrows in Fig. 2(a)] are shown in Figs. 2(f) and 2(h), respectively. Figures 2(g) and 2(i) show the second-derivative plots of these spectra with respect to energy. For cut 1, two shallow electron bands are seen near E_F . For cut 2, one can see two linear bands intersecting each other near E_F , which results from the band folding due to the SDW order.

ARPES spectra observed in the PM phase well above $T_s = 142$ K are shown in Fig. 3. Figure 3(a) shows in-plane FS mapping at 200 K. The FSs clearly changed in shape: δ electron pockets near the X point disappeared and electron pockets appeared at the X and Y points. ARPES spectra along cut 1 for $T = 150$ K and 200 K are shown in Figs. 3(b) and 3(c), respectively. Figures 3(d) and 3(e) show their second-

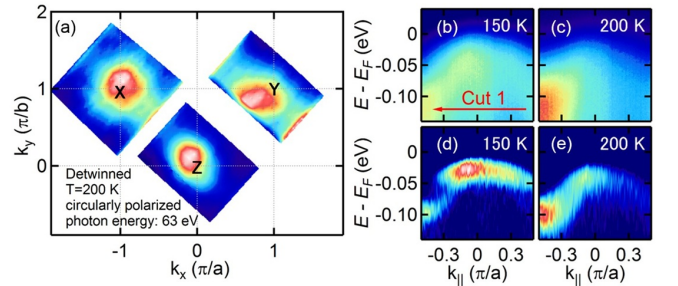


FIG. 3. ARPES spectra of BaFe_2As_2 in the paramagnetic (PM) tetragonal phase. (a) Fermi-surface mapping. The spectra were taken at $T = 200$ K. (b), (c) Energy-momentum plots along cut 1 in Fig. 1(a) for $T = 150$ K and 200 K. (d), (e) Second-derivative plots of (b) and (c) with respect to energy.

derivative plots. In comparison with the spectra in the AFO phase [Figs. 2(f) and 2(g)], the shallow electron-like bands near E_F became increasingly difficult to observe with temperature and that only hole bands centered at the Z point remained at 200 K.

In order to see predicted changes in the band dispersions between the AFO phase and the PM phase, we have performed DFT calculations on BaFe_2As_2 in the PM and AFM states, as shown in Fig. 4. Red and blue band dispersions are those in the PM and AFM states, respectively. Figures 4(a) and (d) show calculated band structures along the Z-X(Γ) direction, Figs. 4(b) and (e) cut 1, and Figs. 4(c) and (f) cut 2. Cut 2

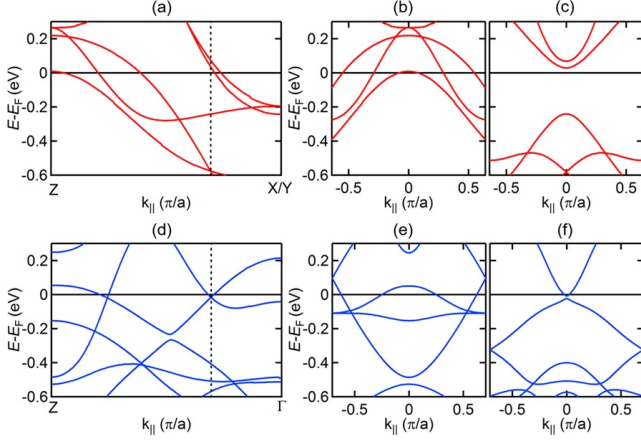


FIG. 4. DFT-GGA calculation of the band structures of BaFe_2As_2 . (a) (d) Band structures of the PM and AFM states, respectively, along the Z-X lines. The Z-X line is perpendicular to cuts 1 and 2. (b), (e) Calculated band structure of the PM and AFM states, respectively, along cut 1. The center of cuts correspond to the Z point and cuts are perpendicular to the Z-X line. (c), (f) Calculated results for cut 2 in the PM and AFM states, respectively. Cut 2 is parallel to cut 1 and crosses the Dirac point indicated by the broken line in (a) and (d).

shown in Figs. 4(c) and 4(f) crosses the Z-X(Γ) line at the dotted line positions shown in Figs. 4(a) and 4(d). Note that the Γ point in the AFM BZ is equivalent to the X/Y point in the PM BZ. In the PM state, one can see three hole bands centered at the Z point and two electron bands centered at the X/Y point [Figs. 4(a) and (b)]. In the AFM state, original bands are hybridized with folded bands and form a complicated band structure [Figs. 4(d)-(f)]. One can see two crossing points near E_F in Fig. 4(d), which are formed by an original hole band and a folded electron band. Since the parities of the two bands are different on the high-symmetry line, they cannot hybridize with each other there. Indeed, in Figs. 4(d) and (f), it is clear that two bands cross each other near E_F . This means that a Dirac cone should be formed near the Fermi level due to the band folding. The calculated band structure for the AFM state is in agreement with the Dirac-cone-like band dispersion observed in our ARPES measurements, indicating that the band structure observed in the present experiment is the intrinsic electronic structure of the AFO phase.

To investigate the electronic structure in the electronic nematic phase, we have performed temperature-dependent measurement of the Dirac-cone band at various temperatures across $T_s = 142$ K and $T^* \sim 170$ K. Figure 5(a) shows E_B versus k plots around the apex of the Dirac cone between $T = 100$ K and 200 K. The linear band crossing can be seen at 100 K as in the case of 20 K. As the temperature increases, the Dirac cone is gradually weakened but persists above $T_N \simeq T_s = 142$ K, and eventually vanishes around $T^* \sim 170$ K. For quantitative comparison, momentum distribution curve (MDC) integrated within the binding energies from 10 meV to 20 meV [Fig. 5(a)] are shown in Fig. 5(b). The figure clearly shows that the Dirac cone gradually weakens upon heating but persists above T_s . Figure 5(c) shows the

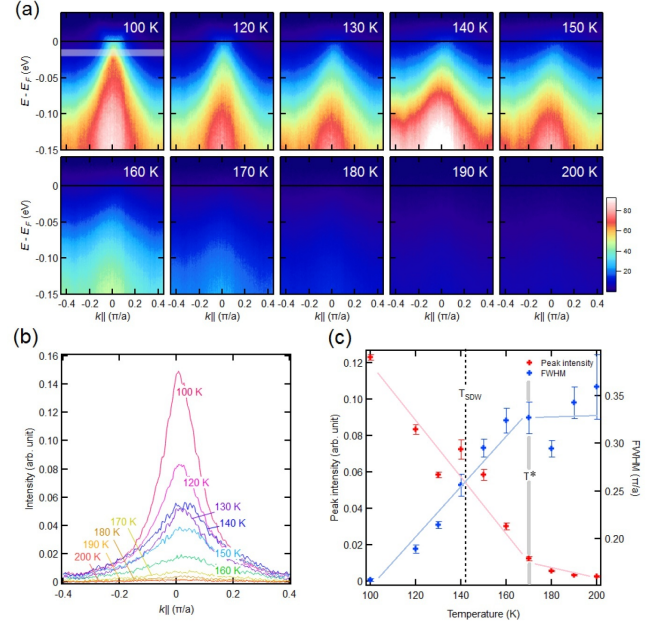


FIG. 5. Temperature dependence of the Dirac-cone feature in ARPES spectra. (a) Evolution of ARPES spectra of BaFe_2As_2 with temperature. Spectra from 100 K to 200 K are taken along cut 2 shown in Fig. 2(a). The spectra have been divided by the FermiDirac function. (b) Temperature evolution of the momentum distribution curve (MDC) for the binding energies from 10 meV to 20 meV. (c) Temperature dependence of the MDC peak intensity and width.

temperature dependence of the peak intensity obtained by integrating the MDC peak from 10 to 20 meV below E_F . As the temperature increases, the peak intensity gradually decreases. We have also plotted the full width at half maximum (FWHM) of the MDC peak in Fig. 5(c). The width significantly increases around T_s upon heating and saturates around ~ 160 K, suggesting that change of the electronic structure associated with the phase transition persists well above T_s . The weak strain by the detwinning is known to induce finite nematicity up to ~ 160 K [33], but cannot explain the band-folding effect observed in the present study.

The present results suggest that short-range SDW or dynamical SDW of the stripe type persists up to $\sim T^*$ or that some electronic order (or short-range order) which has the same periodicity as the stripe-type SDW order remains above $T_N = T_s$. As for the possibility of short-range or dynamical SDW, only nematic spin correlations, i.e., the elongation of Bragg spots along one direction, has been reported above $T_N = T_s$ by inelastic neutron scattering studies of detwinned crystals [34, 35]. As for the orbital degrees of freedom of the electronic structure, $\pm O_{xz}$ -antiferro-quadrupole order ($xy \pm xz$ orbital order) has been theoretically proposed as a possible antiferro-orbital order in the 122-type Fe pnictides (because of the proximity of the Fe xy orbital to the Fermi level compared to the 11-type ones) [26]. This orbital order has the same spatial periodicity as the stripe-type SDW. In Fe-based superconductors, it has been considered that the orbital degrees of freedom play an important role because the

six electrons of Fe^{2+} occupy five $3d$ orbitals located near the Fermi level, and it is likely that antiferro-orbital order exists in the electronic nematic phase. According to the previous ARPES study of BaFe_2As_2 [16], broken C_4 rotational symmetry of the electronic structure persists up to $T \sim 170$ K indicating the presence of *ferro*-orbital order. Our results indicate that in addition to the ferro-orbital order, there also exists *antiferro*-orbital ordering in the electronic nematic phase.

ACKNOWLEDGMENT

We are grateful to H. Kontani, S. Onari, and Y. Yamakawa for valuable discussion. We thank D. Hirai for his help in resistivity measurements. Transport measurements were also performed using facilities at the Cryogenic Research Center,

the University of Tokyo. The experiment at Photon Factory was approved by the Photon Factory Program Advisory Committee (Proposals No. 2015S2-003). This work was partly supported by the National Science and Technology Council of Taiwan under Grant No. 113-2112-M-007-033 and by the Japan Society for the Promotion of Science under Grant No. JP22K03535. A.F. acknowledges the support of the Yushan Fellow Program and the Center for Quantum Science and Technology within the framework of the Higher Education Sprout Project under the Ministry of Education of Taiwan.

DATA AVAILABILITY

All data generated or analyzed during this study are available from the corresponding author upon reasonable request.

-
- [1] Q. Huang, Y. Qiu, W. Bao, M. A. Green, J. W. Lynn, Y. C. Gasparovic, T. Wu, G. Wu, and X. H. Chen, Neutron-diffraction measurements of magnetic order and a structural transition in the parent BaFe_2As_2 compound of FeAs-based high-temperature superconductors, *Phys. Rev. Lett.* **101**, 257003 (2008).
 - [2] A. S. Sefat, R. Jin, M. A. McGuire, B. C. Sales, D. J. Singh, and D. Mandrus, Superconductivity at 22 K in Co-doped BaFe_2As_2 crystals, *Phys. Rev. Lett.* **101**, 117004 (2008).
 - [3] L. J. Li, Y. K. Luo, Q. B. Wang, H. Chen, Z. Ren, Q. Tao, Y. K. Li, X. Lin, M. He, and Z. W. Zhu, Superconductivity induced by Ni doping in BaFe_2As_2 single crystals, *New. J. Phys.* **11**, 025008 (2009).
 - [4] P. C. Canfield, S. L. Bud'ko, N. Ni, J. Q. Yan, and A. Kracher, Decoupling of the superconducting and magnetic/structural phase transitions in electron-doped BaFe_2As_2 , *Phys. Rev. B* **80**, 060501 (2009).
 - [5] S. Jiang, H. Xing, G. Xuan, C. Wang, Z. Ren, C. Feng, J. Dai, Z. Xu, and G. Cao, Superconductivity up to 30 K in the vicinity of the quantum critical point in $\text{BaFe}_2(\text{As}_{1-x}\text{P}_x)_2$, *J. Phys.: Condens. Matter* **21**, 382203 (2009).
 - [6] N. Ni, A. Thaler, J. Q. Yan, A. Kracher, E. Colombier, S. L. Bud'ko, P. C. Canfield, and S. T. Hannahs, Temperature versus doping phase diagrams for $\text{Ba}(\text{Fe}_{1-x}\text{TM}_x)_2\text{As}_2$ (TM=Ni, Cu/Co) single crystals, *Phys. Rev. B* **82**, 024519 (2010).
 - [7] S. Kasahara, H. J. Shi, K. Hashimoto, S. Tonegawa, Y. Mizukami, T. Shibauchi, K. Sugimoto, T. Fukuda, T. Terashima, A. H. Nevidomskyy, and Y. Matsuda, Electronic nematicity above the structural and superconducting transition in $\text{BaFe}_2(\text{As}_{1-x}\text{P}_x)_2$, *Nature* **486**, 555 (2012).
 - [8] M. Yi, H. Pfau, Y. Zhang, Y. He, H. Wu, T. Chen, Z. R. Ye, M. Hashimoto, R. Yu, Q. Si, D.-H. Lee, P. Dai, Z.-X. Shen, D. H. Lu, and R. J. Birgeneau, Nematic energy scale and the missing electron pocket in FeSe, *Phys. Rev. X* **9**, 041049 (2019).
 - [9] T. Kondo, R. M. Fernandes, R. Khasanov, C. Liu, A. D. Palczewski, N. Ni, M. Shi, A. Bostwick, E. Rotenberg, J. Schmalian, S. L. Bud'ko, P. C. Canfield, and A. Kaminski, Unexpected fermi-surface nesting in the pnictide parent compounds BaFe_2As_2 and CaFe_2As_2 revealed by angle-resolved photoemission spectroscopy, *Phys. Rev. B* **81**, 060507 (2010).
 - [10] L. Liu, T. Mikami, S. Ishida, K. Koshiishi, K. Okazaki, T. Yoshida, H. Suzuki, M. Horio, L. C. C. Ambolode, J. Xu, H. Kumigashira, K. Ono, M. Nakajima, K. Kihou, C. H. Lee, A. Iyo, H. Eisaki, T. Kakeshita, S. Uchida, and A. Fujimori, In-plane electronic anisotropy in the antiferromagnetic orthorhombic phase of isovalent-substituted $\text{Ba}(\text{Fe}_{1-x}\text{Ru}_x)_2\text{As}_2$, *Phys. Rev. B* **92**, 094503 (2015).
 - [11] J.-H. Chu, J. G. Analytis, K. D. Greve, P. L. McMahon, Z. Islam, Y. Yamamoto, and I. R. Fisher, In-plane resistivity anisotropy in an underdoped iron arsenide superconductor, *Science* **329**, 824 (2010).
 - [12] S. Ishida, T. Liang, M. Nakajima, K. Kihou, C. H. Lee, A. Iyo, H. Eisaki, T. Kakeshita, T. Kida, M. Hagiwara, Y. Tomioka, T. Ito, and S. Uchida, Manifestations of multiple-carrier charge transport in the magnetotstructurally ordered phase of BaFe_2As_2 , *Phys. Rev. B* **84**, 184514 (2011).
 - [13] M. Nakajima, T. Liang, S. Ishida, Y. T. K. Kihou, C. H. Lee, A. Iyo, H. Eisaki, T. Kakeshita, T. Ito, and S. Uchida, Unprecedented anisotropic metallic state in undoped iron arsenide BaFe_2As_2 revealed by optical spectroscopy, *Proc. Natl. Acad. Sci. U. S. A.* **108**, 12238 (2011).
 - [14] A. Dusza, A. Lucarelli, F. Pfuner, J.-H. Chu, I. R. Fisher, and L. Degiorgi, Anisotropic charge dynamics in detwinned $\text{Ba}(\text{Fe}_{1-x}\text{Co}_x)_2\text{As}_2$, *Europhys. Lett.* **93**, 37002 (2011).
 - [15] J. Zhao, D. T. Adroja, D.-X. Yao, R. Bewley, S. Li, X. F. Wang, G. Wu, X. H. Chen, J. Hu, and P. Dai, Spin waves and magnetic exchange interactions in CaFe_2As_2 , *Nat. Phys.* **5**, 555 (2009).
 - [16] M. Yi, D. Lu, J.-H. Chu, J. G. Analytis, A. P. Sorini, A. F. Kemper, B. Moritz, S.-K. Mo, R. G. Moore, M. Hashimoto, W.-S. Lee, Z. Hussain, T. P. Devereaux, I. R. Fisher, and Z.-X. Shen, Symmetry-breaking orbital anisotropy observed for detwinned $\text{Ba}(\text{Fe}_{1-x}\text{Co}_x)_2\text{As}_2$ above the spin density wave transition, *Proc. Natl. Acad. Sci. U. S. A.* **108**, 6878 (2011).
 - [17] S. Ishida, M. Nakajima, T. Liang, K. Kihou, C. H. Lee, A. Iyo, H. Eisaki, T. Kakeshita, Y. Tomioka, T. Ito, and S. Uchida, Anisotropy of the in-plane resistivity of underdoped $\text{Ba}(\text{Fe}_{1-x}\text{Co}_x)_2\text{As}_2$ superconductors induced by impurity scattering in the antiferromagnetic orthorhombic phase, *Phys. Rev. Lett.* **110**, 207001 (2013).
 - [18] S. Ishida, M. Nakajima, T. Liang, K. Kihou, C. H. Lee, A. Iyo, E. H. T. Kakeshita, Y. Tomioka, T. Ito, and S. Uchida, Effect of doping on the magnetotstructural ordered phase of iron ar-

- senides: A comparative study of the resistivity anisotropy in doped BaFe_2As_2 with doping into three different sites, *J. Am. Chem. Soc.* **135**, 3158 (2013).
- [19] A. J. Achkar, M. Zwiebler, C. McMahon, F. He, R. Sutarto, I. Djianto, Z. Hao, M. J. P. Gingras, M. Hucker, G. D. Gu, A. Revcolevschi, H. Zhang, Y.-J. Kim, J. Geck, and D. G. Hawthorn, Nematicity in stripe-ordered cuprates probed via resonant x-ray scattering, *Science* **351**, 576 (2016).
- [20] K. Ishida, S. Hosoi, Y. Teramoto, T. Usui, Y. Mizukami, K. Itaka, Y. Matsuda, T. Watanabe, and T. Shibauchi, Divergent nematic susceptibility near the pseudogap critical point in a cuprate superconductor, *J. Phys. Soc. Jpn.* **89**, 064707 (2020).
- [21] S. Nakata, M. Horio, K. Koshiishi, K. Hagiwara, C. Lin, M. Suzuki, S. Ideta, K. Tanaka, D. Song, Y. Yoshida, H. Eisaki, and A. Fujimori, Nematicity in a cuprate superconductor revealed by angle-resolved photoemission spectroscopy under uniaxial strain, *npj Quantum Mater.* **6**, 86 (2021).
- [22] F. Ronning, T. Helm, K. R. Shirer, M. D. Bachmann, L. Balicas, M. K. Chan, B. J. Ramshaw, R. D. McDonald, F. F. Balakirev, M. Jaime, E. D. Bauer, and P. J. W. Moll, Electronic in-plane symmetry breaking at field-tuned quantum criticality in CeRhIn_5 , *Nature* **548**, 313 (2017).
- [23] T. Shimojima, Y. Suzuki, T. Sonobe, A. Nakamura, M. Sakano, J. Omachi, K. Yoshioka, M. Kuwata-Gonokami, K. Ono, H. Kumigashira, A. E. Böhmer, F. Hardy, T. Wolf, C. Meingast, H. v. Löhneysen, H. Ikeda, and K. Ishizaka, Lifting of xz/yz orbital degeneracy at the structural transition in detwinned fese, *Phys. Rev. B* **90**, 121111 (2014).
- [24] C.-C. Lee, W.-G. Yin, and W. Ku, Ferro-orbital order and strong magnetic anisotropy in the parent compounds of iron-pnictide superconductors, *Phys. Rev. Lett.* **103**, 267001 (2009).
- [25] M. Yoshizawa, D. Kimura, T. Chiba, S. Simayi, Y. Nakanishi, K. Kihou, C. H. Lee, A. Iyo, H. Eisaki, M. Nakajima, and S. i. Uchida, Structural quantum criticality and superconductivity in iron-based superconductor $\text{Ba}(\text{Fe}_{1-x}\text{Co}_x)_2\text{As}_2$, *J. Phys. Soc. Jpn.* **81**, 024604 (2012).
- [26] H. Kontani, T. Saito, and S. Onari, Origin of orthorhombic transition, magnetic transition, and shear-modulus softening in iron pnictide superconductors: Analysis based on the orbital fluctuations theory, *Phys. Rev. B* **84**, 024528 (2011).
- [27] Y. Kim, H. Oh, C. Kim, D. Song, W. Jung, B. Kim, H. J. Choi, C. Kim, B. Lee, S. Khim, H. Kim, K. Kim, J. Hong, and Y. Kwon, Electronic structure of detwinned BaFe_2As_2 from photoemission and first principles, *Phys. Rev. B* **83**, 064509 (2011).
- [28] P. Blaha, K. Schwarz, G. K. H. Madsen, D. Kvasnicka, and J. Luitz, *WIEN2k, An Augmented Plane Wave + Local Orbitals Program for Calculating Crystal Properties* (Technische Universität Wien, Vienna, Austria, 2001).
- [29] M. Rotter, M. Tegel, D. Johrendt, I. Schellenberg, W. Hermes, and R. Pöttgen, Spin-density-wave anomaly at 140 K in the ternary iron arsenide BaFe_2As_2 , *Phys. Rev. B* **78**, 020503 (2008).
- [30] P. Richard, K. Nakayama, T. Sato, M. Neupane, Y.-M. Xu, J. H. Bowen, G. F. Chen, J. L. Luo, N. L. Wang, X. Dai, Z. Fang, H. Ding, and T. Takahashi, Observation of dirac cone electronic dispersion in BaFe_2As_2 , *Phys. Rev. Lett.* **104**, 137001 (2010).
- [31] T. Terashima, N. Kurita, M. Tomita, K. Kihou, C.-H. Lee, Y. Tomioka, T. Ito, A. Iyo, H. Eisaki, T. Liang, M. Nakajima, S. Ishida, S.-i. Uchida, H. Harima, and S. Uji, Complete fermi surface in BaFe_2As_2 observed via Shubnikov-de Haas oscillation measurements on detwinned single crystals, *Phys. Rev. Lett.* **107**, 176402 (2011).
- [32] One may point out that the hole Fermi surface could not be observed at the Z point by the Shubnikov-de Haas oscillation measurements. However, we consider that the photon energy of 63 eV used in our measurements did not exactly correspond to the Z point, or that k_z -integrated FSs was observed due to momentum resolution. In spite of that, our results are basically the same as the previous study.
- [33] X. Ren, L. Duan, Y. Hu, J. Li, R. Zhang, H. Luo, P. Dai, and Y. Li, Nematic crossover in BaFe_2As_2 under uniaxial stress, *Phys. Rev. Lett.* **115**, 197002 (2015).
- [34] X. Lu, J. T. Park, R. Zhang, H. Luo, A. H. Nevidomskyy, Q. Si, and P. Dai, Nematic spin correlations in the tetragonal state of uniaxial-strained $\text{BaFe}_{2-x}\text{Ni}_x\text{As}_2$, *Science* **345**, 657 (2014).
- [35] H. Man, X. Lu, J. S. Chen, R. Zhang, W. Zhang, H. Luo, J. Kulda, A. Ivanov, T. Keller, E. Morosan, Q. Si, and P. Dai, Electronic nematic correlations in the stress-free tetragonal state of $\text{BaFe}_{2-x}\text{Ni}_x\text{As}_2$, *Phys. Rev. B* **92**, 134521 (2015).